Journal of Energy Storage 72 (2023) 108418

Contents lists available at ScienceDirect

Journal of Energy Storage

journal homepage: www.elsevier.com/locate/est

Research papers

A study on the effect of cell spacing in large-scale air-cooled battery thermal management systems using a novel modeling approach

Amin Moosavi *, Anna-Lena Ljung, T. Staffan Lundström

Division of Fluid Mechanics, Department of Engineering Sciences and Mathematics, Luleå University of Technology, 971 87 Luleå, Sweden

ARTICLE INFO

Keywords:
Battery thermal management system
Cylindrical lithium battery
Analytical model
URANS model
Spacing effect

ABSTRACT

Recent studies have revealed that effective thermal management systems are necessary to maintain the performance, lifespan, and safety of lithium battery systems. A unique and novel modeling approach is presented in this work with the aim of estimating the thermal performance of air-based cooling systems for large-scale lithium battery packages. The overall model consists of sub-models, including an analytical model for battery cells and a numerical heat and flow model for the battery module, which are validated against experimental data and empirical correlations, respectively. The chosen approach implies that the sub-models can operate independently, allowing accurate transient simulations with reduced processing time. The model is employed to evaluate the effect of cell spacing on the thermal performance of an air-cooled battery system designed for a hybrid electric vehicle. The results demonstrate that the maximum temperature within the cells positively correlates with transverse and longitudinal pitch ratios; however, the maximum temperature difference in the module has a negative correlation with these pitch ratios. In contrast, temperature uniformity shows non-monotonic behavior, making it an applicable criterion to balance between temperature rise and thermal gradients. Moreover, considerable temperature non-uniformity is noted in the early rows, which becomes less significant as pitch ratios decrease.

1. Introduction

There is no doubt that the sustainable development of societies relies on the green energy transition [1]. Accordingly, a serious international effort is currently in progress to accelerate the transition toward green energy sources [2] and raise the global capacity of electrical energy production. However, with the growing trend of electrification and reliance on electricity, energy storage has emerged as a new issue [3]. In comparison to other energy storage systems, lithium batteries have gained considerable attention due to their versatility and preferred properties, including high energy content and fast charging capacity. Despite their superiority, lithium batteries are vulnerable to severe operating temperatures. Low temperatures may cause poor energy release, and high temperatures may lead to thermal runaway and explosion [4]. Considering the global interest in mass production and the widespread use of lithium batteries in electric vehicles [5], it is evident that efficient thermal management systems need to be developed for lithium batteries. Various techniques have been used to keep the operating temperature of lithium battery packages within the optimal range [6]. According to the cooling medium, the techniques may generally be divided into three categories: air-based, liquid-based, and PCM-based [7]. Each technique has strengths; however, the simple design, lightweight, absence of leakage risk, and most significantly low manufacturing costs of air-based battery thermal management systems (BTMSs) have recently boosted interest in their industrial applications, particularly for prismatic battery packages [8].

Thermal management of cylindrical battery packages by air-based techniques is relatively challenging due to the small surface area of the cells for heat convection and poor thermal conductivity inside the jellyrolls. Nonetheless, the effectiveness of air-based BTMSs for cylindrical battery packages has been the subject of several studies [9] due to the high energy density and low manufacturing costs of cylindrical lithium battery cells. Indeed, the low thermal conductivity and heat capacity of air restrict the efficient performance of air-based BTMSs. There are two strategies to tackle this issue: modifying the heat transfer mechanism or enhancing the design. The typical strategy to modify the heat transfer mechanism relies on the principle of evaporation, and increasing the humidity of the air can trigger the evaporation mechanism to assist in the heat removal process. Based on a similar concept, mist cooling for BTMSs can enhance the heat transfer rate of cells up to 45% when compared to dry air-induced convection [10]. However, at low temperatures and high relative humidity conditions, the performance of mist-cooling BTMSs becomes unsteady [11].

* Corresponding author.
E-mail address: amin.moosavi@ltu.se (A. Moosavi).

https://doi.org/10.1016/j.est.2023.108418
Received 27 February 2023; Received in revised form 15 June 2023; Accepted 16 July 2023
Available online 5 August 2023

Nomenclature

List of symbols

A	Circumferential heat transfer area for the battery cell [m^2]
D	Battery cell diameter [m]
F	Row-to-row variation ratio of heat transfer coefficient
H	Height of the cell [m]
h	Heat transfer coefficient [$Wm^{-2}K^{-1}$]
I	Electric current [A]
L	Center-to-center distance between the battery cells [m]
N	Row index
n	Number of battery cells per row
P	Pressure [atm]
$\dot{q}$	Heat generation [W]
R	Electrical resistance [Ω]
r	Radius of the cell [m]
SL	Longitudinal pitch ratio
ST	Transverse pitch ratio
T	Temperature [K]
t	Time [s]
U	Velocity [m s^{-1}]

Greek letters

Δ	difference of the variable
ρ	Density [kg m^{-3}]
σ	Standard deviation of the variable

Subscripts

c	Battery cell
$down$	Downstream
f	Cooling fluid
g	Based on the shortest gap distance between the battery cells
irr	Irreversible
L	Longitudinal
max	Maximum
ref	Reference
rev	Reversible
$surf$	Surface
T	Transverse
tot	Total
up	Upstream

Superscripts

N	Row index

Acronyms

$2D$	Two-Dimensional
$3D$	Three-Dimensional
$BTMS$	battery thermal management system
CFD	computational fluid dynamics
DES	Detached Eddy Simulation
LES	Large Eddy Simulation
Nu	Nusselt number
PCM	phase-change material
Re	Reynolds number
$URANS$	Unsteady Reynolds-averaged Navier–Stokes

In air-based BTMSs where forced convection is the major heat transfer mechanism, many studies have been done to enhance the design of airflow channels for improving the heat transfer rate and providing a homogeneous temperature condition between the battery cells [8]. It has been observed that increasing confinement within the flow channel reduces the temperature in battery cells, regardless of the temperature of the air being supplied [12]. Moreover, the use of confining fins in cross-flow BTMSs has been observed to significantly enhance the heat transfer efficiency of the system [13]. The integration of this concept with the counter-axial flow cooling approach has resulted in the development of the reversed layer cooling method [14], which displays improved temperature uniformity across the battery package. However, this idea results in a more complicated design, an increased pressure drop, and a higher energy consumption rate. Furthermore, it has been found that the flow channel designs with increased confinement lose their benefits at high air flow rates [15] and even increase non-uniformity in axial flow cooling systems [16]. In general, air-based BTMSs with cross-flow over the cells provide superior thermal performance than axial flow [17]; nevertheless, the lack of temperature uniformity in large-scale systems makes them inefficient for high-performance battery systems. Including an inlet plenum in the cross-flow battery cooling systems is a new technique for regulating temperature distribution throughout battery cells. Using an intake plenum to supply fresh air for the inner rows can result in a 9% decrease in temperature rise and a 39% improvement in temperature uniformity throughout the battery cells [18]. Although the approach may be sound, it causes a considerable pressure drop in the system and necessitates a specific design for battery packages with varying arrangements and spacing. In systems with pressure drop constraints, the reciprocating air flow battery cooling system may be an alternate design that dramatically reduces the thermal gradient in the battery package by 72% at the cost of lower thermal efficiency [19]. The effectiveness of all mentioned battery thermal management methods relies significantly on the layout and spacing of the battery cells within the flow channel. Overall, studies have revealed that a line-type layout for battery cells outperforms square-type and ring-type layouts in terms of thermal performance [20]. The battery cells in the line-type layout can also be arranged in a variety of ways, including in-line, staggered, and zigzag arrangements. The current state of the literature lacks a clear consensus regarding the ideal arrangement for air-based BTMSs. While earlier studies have emphasized the advantages of an in-line arrangement [21,22], more recent research reveals that a staggered arrangement may be more efficient [23,24].

This ambiguity means that air-based BTMSs with identical layouts may perform differently for battery packages with varied specifications and operating conditions, and so on. Moreover, it emphasizes the necessity of customizing the design of BTMSs for battery packages based on their specifications, requirements, and application. This approach demands comprehensive parametric studies, making it almost impossible to scrutinize with physical experiments. Numerical simulation based on finite volume or finite element methods might be a proper research tool for this purpose; however, the following considerations can make the simulation of a large-scale battery system problematic in terms of computational costs:

- The generation of heat in a battery cell is a time-dependent problem requiring transient modeling over a long time period that might range from several minutes to a few hours, depending on the charging/discharging rate (C-rate).
- The accurate simulation of flow behavior surrounding the battery cells necessitates a transient simulation with small time steps and computationally expensive models.

Table 1
Specifications of the battery cell [26].

Specification [unit]	Value
Diameter [mm]	21
Height [mm]	70
Specific heat capacity [J/kg – K]	1000
Radial thermal conductivity [W/m – K]	1
Axial thermal conductivity [W/m – K]	25
Tangential thermal conductivity [W/m – K]	25
Nominal Voltage [V]	3.56
Nominal capacity [Ah]	3.2
Internal resistance [mΩ]	50

- A large-scale battery system can contain hundreds or even thousands of battery cells, making the expense of running a full-size simulation unacceptably high.

It is clear that the combination of the long simulation period, small time steps, and a large domain size poses an extraordinary computational burden for the full-size simulation of large-scale battery systems. Hence, a practical and efficient modeling approach is necessary to study the thermal performance of large-scale battery thermal management systems.

To tackle this issue, this work proposes a simplified modeling approach based on the combination of numerical and analytical models for the thermal evaluation of an air-based battery thermal management system. The modeling approach is built from three sub-models: an analytical model to predict thermal behavior within the battery cells; a computational fluid dynamics (CFD) model to predict flow behavior over the battery cells in the inner rows; and a system of equations to estimate thermal evolution throughout the battery cooling system. The following illustrates the potential of the approach and its relevance to the challenges mentioned, as well as how it reduces computational costs for system simulation.

- The individual model for battery cells enables the exclusion of cells from the computational domain while employing the analytical method to predict the temperature field for each cell.
- The sub-models can run independently and are coupled together using the circumferential heat transfer coefficients. This technique implies that tiny time steps and sophisticated turbulence models can be employed during the CFD simulations while still predicting the thermal behavior of battery cells over long charging/discharging periods.
- The system of equations enables us to estimate thermal evolution along large-scale battery systems by only modeling a smaller domain in the periodic region.

Besides, the modeling approach is employed to study the thermal performance of an air-based cross-flow cooling system with a staggered arrangement of the battery cells designed for a hybrid electric vehicle. The effect of transverse and longitudinal pitch ratios on the thermal behavior of the battery cells and temperature uniformity within the battery module is investigated to determine optimal pitch ratios for the battery system.

2. Model development

2.1. Illustration of physical problem

According to our earlier work, 21700 lithium batteries offer better thermal performance compared to other cylindrical battery types [25]. So, the battery package design consists of 21700 lithium batteries to reduce the weight of the additional heat load on the BTMS. The battery specifications are provided in Table 1.

To satisfy the battery package requirement for a hybrid electric vehicle, 83 battery cells are connected in series to provide a nominal voltage of 295 V in a module. The package also consists of 166 cells in two parallel modules, providing a nominal capacity of 1.9 kWh. In the module, the cells are placed in a staggered arrangement with a defined transversal pitch ratio ($ST = \frac{L_T}{D}$) and longitudinal pitch ratio ($ST = \frac{L_L}{D}$), as illustrated in Fig. 1. Thus, the dimensions of the module can be derived using the number of cells and given pitch ratios in the transverse and longitudinal directions.

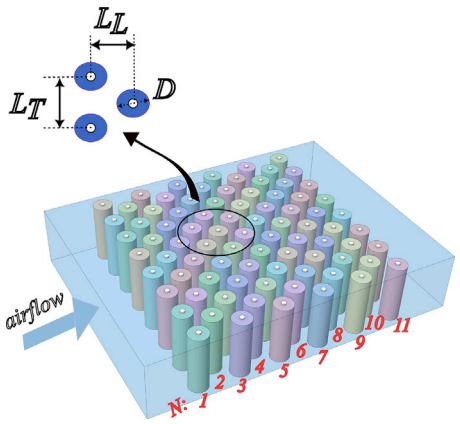

Fig. 1. Schematic view of the battery thermal management system.

Thermal-related problems in a battery depend on the C-rate, which is a unit used to determine the rate of the charging and discharging processes. For instance, a 1 C charging/discharging rate is the current rate at which the battery can be fully charged/discharged in one hour. In this study, battery cells are assumed to experience significant overheating under the extreme condition of a 3 C charging/discharging rate (which means that it takes only 20 min to fully charge/discharge the battery pack). It is possible to control temperature rise within the battery cells using cold airflow; however, the airflow rate and the configuration of the battery cells determine the effectiveness of this approach. To regulate the temperature of the batteries without risking the comfort of the passengers in the cabin, it should be considered that the airflow supply is not limitless and requires a reference value. There are several methods to provide air for the thermal management of the battery package [27]; however, in this study, the passive approach of air supply from the air-conditioned car cabin is chosen. According to the airflow analysis by Zolot et al. [28], a hybrid electric vehicle's airflow rate at a high blower setting is 48.4 [SCFM] at the standard temperature ($T_{standard}$) and pressure ($P_{standard}$) of 293.15 [K] and 1 [atm], respectively. The measurements were conducted at the actual temperature (T_{actual}) and actual pressure (P_{actual}) of 323.15 [K] and 0.81 [atm], respectively. Based on the standard and actual temperature and pressure values, as well as the thermophysical properties of the airflow, provided in Table 2, the following equation may be used to calculate the air mass flow rate ($\dot{m}$):

$$\dot{m} = 47.195 \times 10^{-5} \left(\rho_f \dot{V}\right) \left(\frac{P_{standard}}{P_{actual}}\right) \left(\frac{T_{actual}}{T_{standard}}\right) \quad (1)$$

where $\dot{V}$ is the volumetric flow rate (in [SCFM]). Thus, the rate of conditioned air supplied from the cabin of a hybrid electric vehicle, which is equal to 0.03636 [kg/s], is employed as the reference intake air flow rate to the battery module that is the subject of this study.

2.2. Thermal model for battery cell

To study the thermal behavior of the battery cells, we utilize an analytical model proposed in our earlier research [25]. The model, which is based on the integral transform technique, predicts the temperature rise in a cylindrical battery in an exact and computationally efficient

Table 2
Thermophysical properties of the airflow.

Material	Density [kg/m^3]	Specific heat capacity [J/kg − K]	Thermal conductivity [W/m − K]	Dynamic viscosity [kg/m − s]
Air	1.1696	1006.9	0.0231	1.7981×10^{-5}

manner and demonstrates good agreement with experimental measurements. Details of the developed model and experimental validation are published in Ref. [25] and will not be repeated here.

The model requires a set of input variables, including the thermophysical properties of the battery cell (listed in Table 1), the heat generation rate, and the heat transfer coefficients. We assume that batteries charge/discharge at a constant rate of 3 C and that the majority of the heat is due to irreversible heat ($\dot{q}_{irr}$) generated by internal electrical resistance within the battery cell, with reversible heat ($\dot{q}_{rev}$) accounting for 20% of the irreversible heat [26]. Hence, the rate of heat generation for a cell can be derived from the following equation:

$$\dot{q}_{tot} = \dot{q}_{irr} + \dot{q}_{rev} \tag{2}$$

where,

$$\dot{q}_{irr} = RI^2, \qquad and \qquad \dot{q}_{rev} = 0.2\,\dot{q}_{irr}. \tag{3}$$

The current rate in the above equation can be determined as the multiplication of the nominal capacity of a cell and the charging/discharging rate ($I = nominal\ capacity \times C - rate$). The heat transfer coefficient on the tabs is assumed to be 5 [W/m^2 − K] to mimic the free natural convection. The circumferential heat transfer coefficient is an unknown variable that varies for each cell along the battery module and needs to be fed into the model. Moreover, the model predicts the temperature rise for each cell with respect to a reference temperature. In this study, the reference temperature is defined as the average temperature of the flow on the upstream and downstream sides of the cell ($T_{ref} = \frac{T_{f,up}+T_{f,down}}{2}$). The temperature of the flow on the upstream and downstream sides of the cell, like the circumferential heat transfer coefficient, is an unknown variable that changes for each cell and is dependent on the Reynolds number and cell spacing. To determine these unknown variables, a CFD-based model is employed as described in the following section.

2.3. Heat and flow model for battery module

Flow through a large-scale battery module may be subject to various sources of instabilities, particularly in the flow transition region [29]. However, a few early rows of the cell are enough to achieve periodic flow with a constant heat transfer coefficient on the cells [30]. The difference in heat transfer coefficient between the early and latter rows of cells depends on the Reynolds number, arrangement of the cells, and pitch ratios. In the staggered arrangement, it is observed that the row-to-row variation of the heat transfer coefficient is independent of pitch ratios and only depends on the Reynolds number [31]. The row-to-row variation of the heat transfer coefficient for a staggered arrangement is shown in Fig. 2, where N and F denote the row number and the ratio of the heat transfer coefficient on each row of the cell to the cell in the periodic region ($F = h^{(N)}/h^{(20)}$, see Fig. 2), respectively. It is evident that beyond the fourth row, the variation of the heat transfer coefficient becomes insignificant, which is corroborated by other authors [30,32].

With the help of this knowledge, the heat coefficient can be estimated for all rows of cells using the heat transfer coefficient for the cell located in the periodic region. The CFD-based model is now used to determine the heat transfer coefficient for the battery modules with different geometries. The study domain consists of a 2 × 2 periodic domain (depicted in Fig. 3(a)) with traverse pitch ratio and longitudinal pitch ratio changing from 1.244 to 2.074 and 0.622 to 1.452, respectively, representing typical spacing in the majority of studies for BTMSs.

To produce a high-quality grid for the CFD study (see Fig. 3), structured hexahedral meshes with $y^+ \sim 1$ are generated in ANSYS ICEM CFD v20.1. Considering the flow periodicity in the study region, the periodic boundary conditions are imposed in all directions with a constant mass flow rate in the x-direction. Air with constant thermophysical properties (listed in Table 2) is employed as the coolant flow, and a constant heat flux corresponding to the rate of heat generation in the battery cells is applied as a heat source.

According to the recent study by Moosavi et al. [33], the thermal performance of a wall-bounded cross-flow heat exchanger, like the battery cooling system utilized in this work, can be assessed using a 2D Unsteady Reynolds-Averaged-Navier–Stokes (URANS) model if the aspect ratio of the cells is greater than two, the average heat transfer coefficient is of interest, and the thermal conductivity along the height of the cells is more significant than in the radial direction. It is so because, in a wall-bounded cross-flow heat exchanger, the average circumferential heat transfer coefficient for a thermal cell with an aspect ratio greater than two remains constant despite significant variations in the local heat transfer coefficient. Furthermore, compared to the temperature gradient in the radial direction, the result of local heat transfer coefficient variations on the temperature gradient in the tangential and axial directions is negligible due to considerable thermal conductivity in those directions. Based on the assumptions that the battery cells used in this study have an aspect ratio of 3.33, the analytical model requires the average heat transfer coefficient over the cells, and the axial thermal conductivity is 25 times greater than the radial thermal conductivity, it is possible to lower the computational burden of the CFD model by reducing it from a 3D to a 2D model. Therefore, all simulations have been carried out using the two-dimensional Unsteady Reynolds-Averaged-Navier–Stokes (URANS) model in ANSYS FLUENT v20.1. Moreover, the accuracy of URANS models is significantly affected by the selection of the turbulence model. It has been observed that the URANS model with the k–kl–ω transition turbulence models can produce findings comparable to LES and DES, and by taking computational cost into account, this choice can be optimal for assessing cross-flow over circular cylinders [33]. Hence, the k–kl–ω transition model is applied for the turbulence modeling to reliably reflect turbulence characteristics while remaining computationally efficient. QUICK and bounded second-order implicit schemes are used for spatial and temporal discretization, respectively. The time step for each simulation is determined as $\Delta t = \frac{\Delta t^+ D}{U_g}$ seconds, where $\Delta t^+ = 0.01$ and U_g is the mean streamwise velocity in the smallest gap between the cylinders. When the initial disturbances have dissipated after $\frac{100D}{U_g}$ seconds of simulation time, the necessary data are collected for $\frac{50D}{U_g}$ seconds of sampling time.

Although the aforementioned models can now predict the temperature rise in cells with respect to a reference temperature, the reference temperature remains an unknown variable that needs to be determined for each cell. When the flow passes through the cells, the fluid temperature rises, raising the reference temperature for each row of cells in the process and, as a result, decreasing the heat transfer rate for the cells in the subsequent rows. Indeed, it might be the main reason for the nonuniform temperature distribution among the cells in large battery thermal management systems. To account for this aspect in the current model, the flow temperature throughout the battery module needs to be evaluated. Given that the coolant fluid must absorb the heat loss from the cells, the following system of equations can be applied to estimate the flow temperature on the upstream and downstream sides of each cell along the battery module.

$$\dot{m}c_p\left(T^{(N)}_{down,f} - T^{(N)}_{up,f}\right) = h^{(N)} nA\Delta T^{(N)}_{surf,c}, \qquad N = 1, 2, 3, \ldots, 11 \tag{4}$$

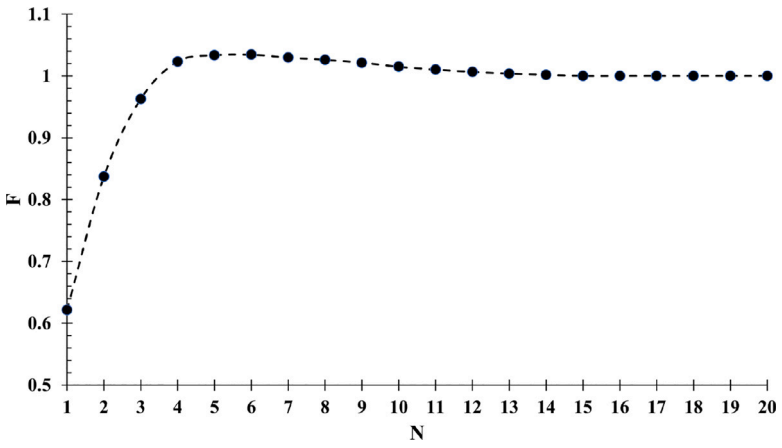

Fig. 2. Row-to-row variation of heat transfer coefficient for staggered arrangement at $Re > 100$ [31].

where,

$$\Delta T_{surf,c}^{(N)} = T_{surf,c}^{(N)} - T_{ref}^{(N)} , \tag{5}$$

and by assuming,

$$T_{ref}^{(N)} = \frac{T_{down,f}^{(N)} + T_{up,f}^{(N)}}{2} , \tag{6}$$

$$T_{down,f}^{(N)} = T_{up,f}^{(N+1)} . \tag{7}$$

In the equations above, N denotes the row number. The $\dot{m}$ (inlet mass flow rate), c_p (specific heat capacity), n (number of battery cells per row), and A (heat transfer area for the cell) are known variables for the problem. The heat transfer coefficient, h, can be determined for each cell using the CFD model and row-to-row variation ratio (F), as described earlier. Moreover, $\Delta T_{surf,c}$ is the difference between the average surface temperature of the cell ($T_{surf,c}$) and the average surrounding flow temperature (T_{ref}), as calculated using the analytical model presented in Section 2.2. Thus, the only variables remaining unknown are $T_{down,f}$ and $T_{up,f}$. To determine these variables, Eqs. (4)–(7) are solved using $T_{up,f}^{(1)}$ as the initial value. In this study, it is assumed that $T_{up,f}^{(1)} = 293.15$ [K] and the defined equations are solved for each cell in order from the first row to the last row. Once $T_{down,f}$ and $T_{up,f}$ are determined for each row, it is straightforward to calculate T_{ref} using Eq. (6). Now, the actual thermal field for each cell along the battery module can be derived by entering the reference value into the analytical model.

3. Results and discussion

3.1. Mesh sensitivity analysis

As mentioned earlier, the CFD assessment of the heat transfer coefficient in the inner region of the battery module is a prerequisite for the proposed modeling approach in this work. Hence, a 2 × 2 cell domain has been chosen to simulate the periodic flow behavior and, consequently, heat transfer in the fully developed flow region of the battery module. Thus, a mesh sensitivity analysis is performed to ensure the reliability of the findings and the computational efficiency of the convergence in the CFD study. The chosen geometry for this analysis has transverse and longitudinal pitch ratios of 1.244 and 1.037, respectively, resulting in the maximum Reynolds number and turbulence intensity. Five computational grids are generated, with mesh resolutions ranging from 7392 to 102392 grid cells. The wall-adjacent initial cell height is always specified to give $y^+ \sim 1$ and expand with a 1.1 growth ratio. Fig. 3 shows a view of the computational grid used for the case with 67472 grid cells.

The Nusselt number predictions by the URANS models with different grid resolutions are used to evaluate the independence of the computational grid. As demonstrated in Fig. 4, the variation in the Nusselt number becomes almost negligible above the 67472 number of grid cells. Hence, the computational grid with 67472 grid cells is chosen as the mesh-independent case for the CFD study, and equivalent mesh parameters are used in the models with other pitch ratios.

3.2. Model validation

The proposed model for the thermal evaluation of an air-based battery thermal management system is a comprehensive model that integrates different sub-models, as illustrated in Section 2. Hence, the validity of each model is scrutinized separately to verify the reliability of the entire model.

The analytical sub-model used for the thermal assessment of a single cylindrical battery cell is already verified using experimental measurements [25]. Under three distinct heating conditions with natural circumferential convection, the model estimate of the maximum temperature rise within a 26650 lithium battery matched the actual data well. The details of the model validation process are described in Ref. [25], and will not be repeated here.

To check the validity of the CFD sub-model described in Section 2.3, the empirical correlation of the average Nusselt number in tube banks suggested by Gnielinski [34] is applied. The model with $ST = 1.244$ and $SL = 1.037$ is used as the study case, and the inlet mass flow rate is varied to produce Reynolds numbers ($Re_g = \frac{\rho U_g D}{\mu}$) ranging from 1000 to 40000.

As demonstrated in Fig. 5, the CFD findings are in good agreement with the empirical correlation, particularly at $Re_g = 2.46 \times 10^4$, which corresponds to the maximum mass flow rate in our under-investigation battery module, where the model shows less than a 3% deviation from the correlation.

3.3. Effect of transverse and longitudinal pitch ratios

The transverse and longitudinal pitch ratios play a significant role in the performance of the BTMS and, consequently, the safe and efficient operation of the battery cells. The trade-off between maximum temperature rise, thermal gradients, compactness, weight, pressure drop, and mass flow rate determines the optimal pitch ratio for a battery thermal management system. Due to system complexity, experimental constraints, and computational expenses, it is often challenging to study the effect of pitch ratios on the performance of battery temperature management systems. However, using the model proposed in this work, it becomes more straightforward to investigate how various pitch ratios affect the performance of the BTMS.

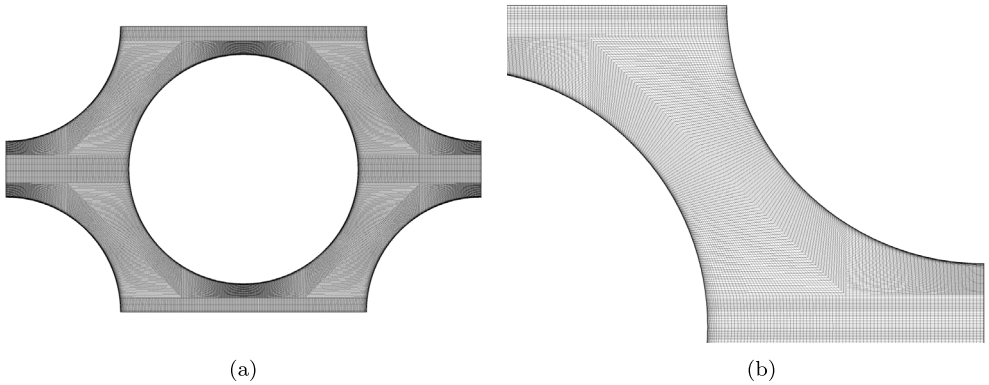

Fig. 3. The view of the computational grid used for the CFD model with $ST = 1.244$, and $SL = 1.037$, (a) Overall view, (b) Enlarged view of the wall-adjacent grid cells.

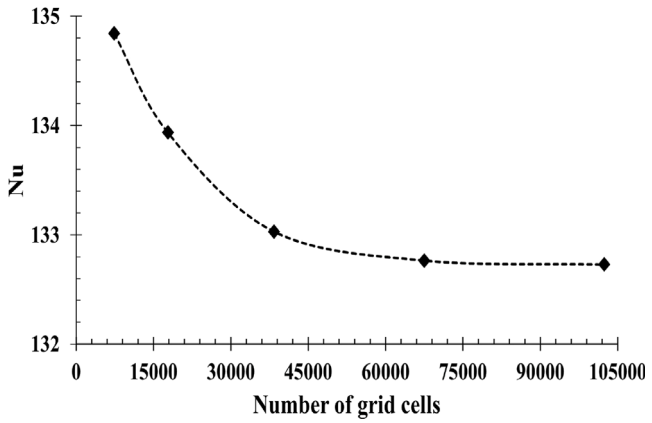

Fig. 4. Mesh sensitivity analysis.

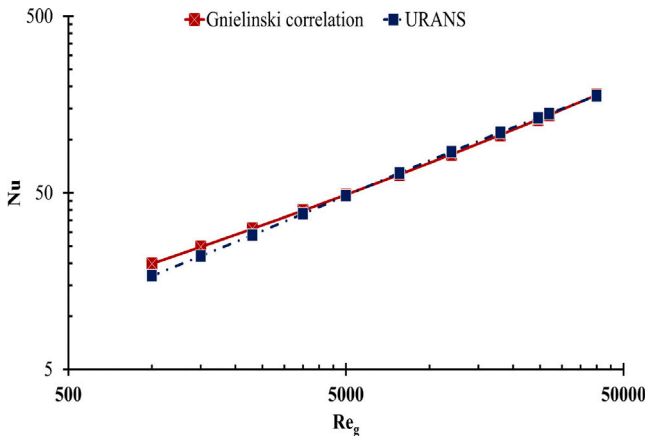

Fig. 5. Nusselt number versus Re_g comparison in CFD (URANS) and Gnielinski correlation.

The influence of transverse and longitudinal pitch ratios on the battery module, illustrated in Section 2.1, is investigated further below. The longitudinal pitch ratio is fixed at 1.037, while the transverse pitch ratio varies from 1.244 to 2.074 to investigate the effect of the transverse pitch ratio. For the longitudinal pitch ratio investigation, the transverse pitch ratio is set at 2.074, and the longitudinal pitch ratio ranges from 0.622 to 1.452. In all cases, the mass flow rate is maintained constant, and it is assumed that air with a constant inlet temperature of 293.15 [K] blows over the battery cells. Based on the discussion from Section 1, a unique CFD model is developed for each case to determine the convective heat transfer rate. Using the area-averaged heat transfer coefficient, the CFD model is coupled to the analytical model and the system of equations to estimate the thermal field of battery cells in each row.

Fig. 6 shows how transverse and longitudinal pitch ratios affect the maximum temperature and thermal gradient in the battery module. As seen in Figs. 6(a)–6(b), the maximum temperature rise in the battery module is positively proportional to the transverse and longitudinal pitch ratios. It indicates that decreasing the transverse and longitudinal gap between the battery cells enhances the thermal performance of the battery thermal management systems and, as a result, reduces the temperature rise within the battery cells.

In the case of transverse pitch ratio, enhanced thermal performance is attributed to an increase in the inlet velocity magnitude caused by a reduction of upstream flow passage area (see Figs. 7(a)–7(b)), which intensifies turbulence and decreases the thickness of the thermal boundary layer over the cells. The proportionality of maximum temperature to transverse pitch ratio appears to be roughly linear; however, in the case of longitudinal pitch ratio, the rate of growth slows down and reaches a plateau (see Fig. 6(b)). It is because the inlet velocity magnitude remains constant when varying the longitudinal pitch ratio, and the intensity of circulation in the wake region, which becomes stable after a certain pitch ratio, is the dominant factor affecting the velocity field surrounding the cells. As shown in Figs. 7(c)–7(d), by reducing the longitudinal distance between cells, the circulation becomes more intense, increasing confinement for the inlet flow passage and forming a high-velocity shear layer over the cell, which consequently enhances the heat transfer rate. These findings might be used to reduce pressure drop in BTMSs with longitudinal pitch ratios larger than 1.3 without risking thermal performance. However, the results demonstrate that the temperature rise is often smaller for compact battery packages.

The maximum surface temperature of the battery cells is a widely used criterion in the literature to assess the effectiveness of battery thermal management systems. It is mainly due to experimental constraints for internal temperature measurements of battery cells or to reduce computational costs. However, as depicted in Fig. 8 for the cell at row 11 in the module with $SL = 1.452$ and $ST = 2.074$, there might be considerable thermal gradients within the cell due to poor thermal conductivity, particularly in the radial direction. Hence, even if the surface temperature is within the acceptable range, the internal temperature at the end of the charging/discharging cycle may rise above the allowed limit. According to the results in Figs. 6(a)–6(b), while maximum surface temperature follows the trend of maximum internal temperature, it underestimates the maximum temperature within the battery cell. In the current study, this underestimation is about 2%; nevertheless, it depends on the battery specifications and should be considered when evaluating the effectiveness of the battery cooling system.

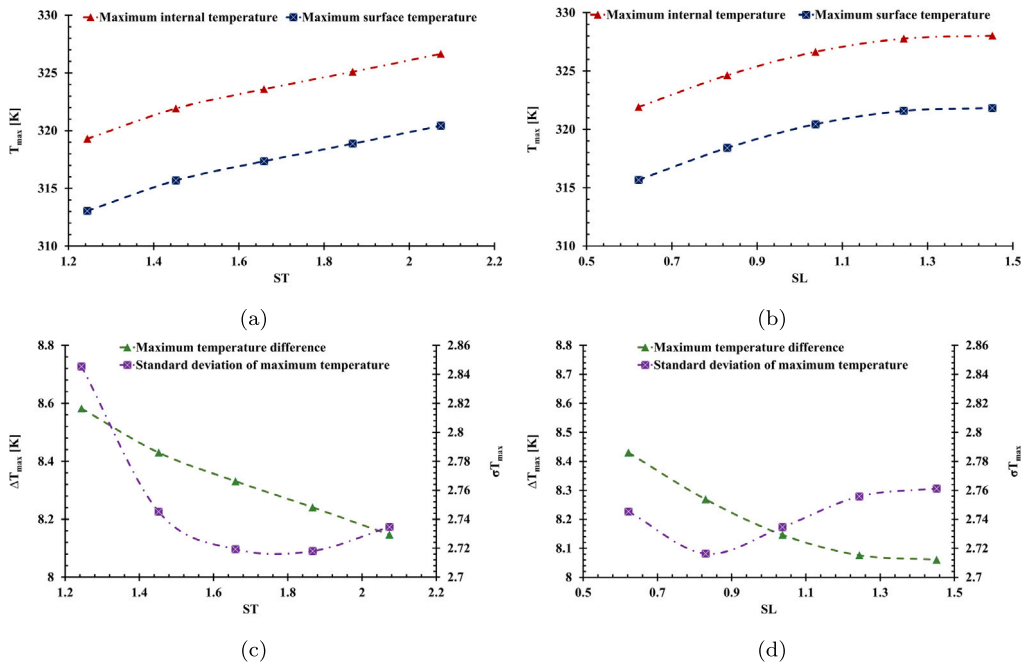

Fig. 6. Effect of transverse pitch ratio on (a) the maximum temperature within the battery module, (b) maximum thermal gradients within the battery module, and effect of longitudinal pitch ratio on (c) the maximum temperature within the battery module, (d) maximum thermal gradients within the battery module.

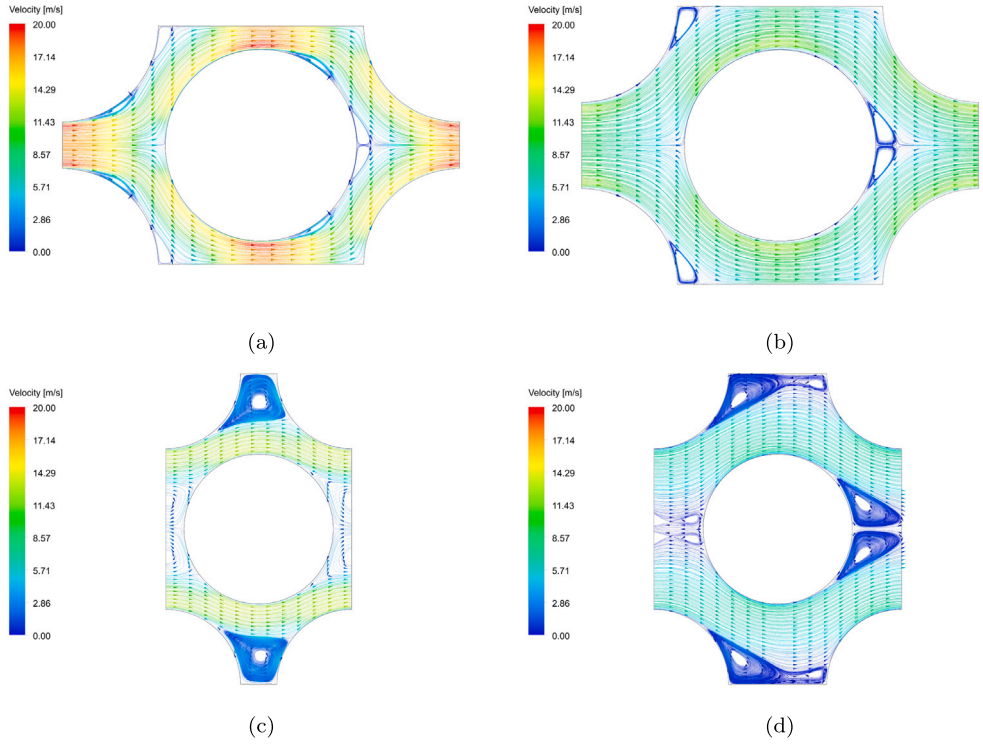

Fig. 7. Velocity streamlines of the periodic flow over the cell at (a) $ST = 1.244$ and $SL = 1.037$, (b) $ST = 1.4518$ and $SL = 1.037$, (c) $ST = 2.074$ and $SL = 0.622$, (d) $ST = 2.074$ and $SL = 0.8296$.

Although the maximum temperature is a critical consideration for the safe operation of most battery packages, it is not the only factor. It is recommended in high-performance battery packages to control temperature gradients in the battery pack, which might induce unbalanced discharging and capacity fade [35]. Hence, the maximum temperature difference within the battery module and temperature uniformity are used as scales to investigate the effect of transverse and longitudinal pitch ratios on temperature gradients. As shown in Figs. 6(c)–6(d), decreasing the transverse and longitudinal gaps between the battery cells increases the maximum temperature difference, which is undesirable. It implies that the optimal pitch ratio depends on the trade-off between maximum temperature rise and maximum temperature difference, which might be determined by the requirements and operating conditions of the battery package. However, temperature uniformity, as another effective factor, can contribute to resolving this uncertainty. The standard deviation of the maximum temperature (σT_{max})

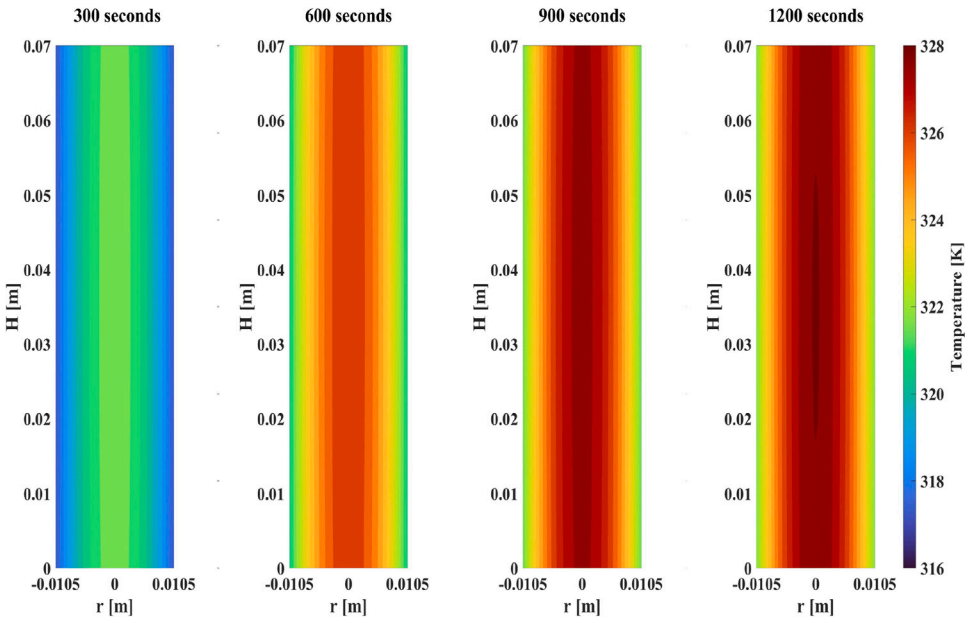

Fig. 8. Temperature field temporal change for a cell at Row 11 in the module with $SL = 1.452$ and $ST = 2.074$.

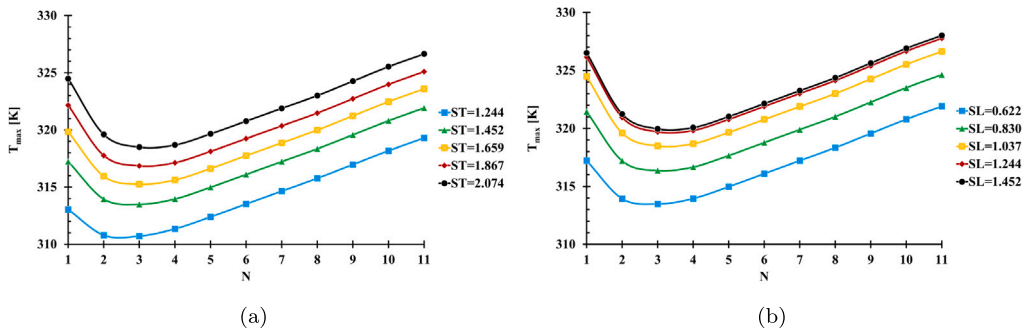

Fig. 9. The row-to-row variation of maximum temperature within the cells throughout the staggered battery module (a) effect of the transverse pitch ratio, (b) effect of the longitudinal pitch ratio.

is employed in this study to evaluate temperature uniformity in the battery module. The effect of transverse and longitudinal pitch ratios on the standard deviation of the maximum temperature is depicted in Figs. 6(c)–6(d). In contrast to the maximum temperature and maximum temperature difference, the standard deviation of the maximum temperature does not show monotonic behavior and has a minimum extremum. It indicates that the battery module has higher temperature uniformity at the transverse and longitudinal pitch ratios of 1.66 and 0.83, respectively.

Temperature non-uniformity in the system can be explained in part by the maximum temperature within cells throughout the battery module. The row-to-row variation of maximum temperature within the cells is presented in Figs. 9(a)–9(b) for the BTMSs with varied transverse and longitudinal pitch ratios.

The results show that in all cases, the maximum temperature throughout the battery module decreases for the initial rows, reaching its lowest point before gradually increasing again. This pattern aligns with the results presented by Saechan et al. [24] and Fan et al. [22] for the staggered arrangement.

As illustrated in Fig. 10, despite a poorer heat transfer rate in the third row compared to the inner rows of the battery pack, the maximum temperature of the battery cell in this row is still lower. The current consequence may be attributed to the fact that the flow temperature in the early rows has not yet risen significantly due to the low heat transfer rate coefficient of the first two cells, resulting in a greater thermal gradient for heat transfer in the third row. The heat transfer coefficient reaches stability after the fourth row, resulting in a continuous temperature rise within the cells throughout the battery module. Moreover, as the transverse and longitudinal pitch ratios increase, the temperature non-uniformity in the early rows becomes more noticeable. It is due to the fact that the larger transverse and longitudinal gaps between the cells, as discussed earlier, lead to a decrease in heat transfer rate in the first two rows, providing a larger thermal gradient for heat transfer rate and less temperature rise for the cells in the third row.

4. Conclusions

In this work, a unique approach is provided for studying the thermal behavior of large-scale BTMSs. The overall model is divided into an analytical battery model and a simplified numerical heat and flow model, allowing for the independent operation of sub-models with fewer computing time limitations and more accurate results. The approach is then used to study the effect of transverse and longitudinal pitch ratios on the thermal performance of an air-based BTMS designed for a hybrid electric vehicle. The following are the main findings of this study:

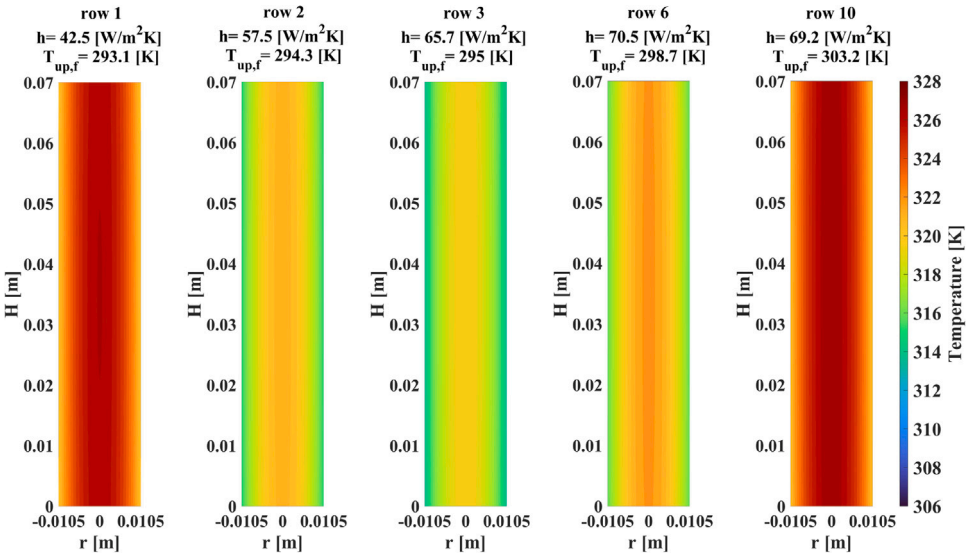

Fig. 10. Temperature field evolution along the module with $SL = 1.452$ and $ST = 2.074$.

- The approach suggested in this paper, which combines numerical and analytical models, is a time-efficient method for estimating heat transfer in large-scale air-cooled battery thermal management systems.
- The maximum temperature and maximum temperature difference within the battery module are positively and negatively proportional to pitch ratios, respectively. Moreover, while the maximum temperature within the module shows almost direct proportionality with the transverse pitch ratio, it demonstrates asymptotic growth behavior with respect to the longitudinal pitch ratio and remains almost constant after 1.3.
- It is observed that the use of maximum surface temperature overestimates cooling effectiveness; nonetheless, it could be used to determine the rate of temperature rise within the battery cells.
- It is found that the temperature uniformity factor could be used as a practical criterion in a trade-off between maximum temperature and maximum temperature difference within the battery module. Based on this, it is determined that the system operates at its optimal thermal condition at transverse and longitudinal pitch ratios of 1.66 and 0.83, respectively.
- Observations reveal that the minimum temperature rise within the battery module consistently occurs in the third row prior to the flow stabilization, regardless of the cell spacing. This is a result of considerable temperature non-uniformity in the early rows of the battery module, which could be alleviated by decreasing the transverse and longitudinal gap distances between the cells.
- Results show that in a staggered battery cooling system with large transverse and longitudinal pitch ratios and a limited number of rows, the maximum temperature is located in the first row. Hence, the simulation of the first three rows could be sufficient to estimate the maximum temperature difference in the system.
- The practical implication of the study is that flow disturbance before the first row is beneficial. Based on the findings, an apparent strategy to reduce temperature non-uniformity in early rows might be to incorporate two dummy rows of battery-shaped cylinders before the actual first row to accelerate flow stabilization. Nevertheless, the feasibility and effectiveness of this approach require further investigation in future studies.

CRediT authorship contribution statement

Amin Moosavi: Conceptualization, Methodology, Software, Validation, Investigation, Writing – original draft. **Anna-Lena Ljung:** Supervision, Writing – review & editing. **T. Staffan Lundström:** Funding acquisition, Supervision, Writing – review & editing.

Declaration of competing interest

The authors declare that they have no known competing financial interests or personal relationships that could have appeared to influence the work reported in this paper.

Data availability

Data will be made available on request.

Acknowledgment

This work was financed by and performed within the framework of StandUp for Energy.

References

[1] T. Güney, Renewable energy, non-renewable energy and sustainable development, Int. J. Sustain. Dev. World Ecol. 26 (5) (2019) 389–397.
[2] H. Heubaum, F. Biermann, Integrating global energy and climate governance: The changing role of the international energy agency, Energy Policy 87 (2015) 229–239.
[3] J.Y. Tsao, E.F. Schubert, R. Fouquet, M. Lave, The electrification of energy: Long-term trends and opportunities, MRS Energy Sustain. 5 (2018).
[4] B. Mao, P. Huang, H. Chen, Q. Wang, J. Sun, Self-heating reaction and thermal runaway criticality of the lithium ion battery, Int. J. Heat Mass Transfer 149 (2020) 119178.
[5] N. Lebedeva, Li-ion Batteries for Mobility and Stationary Storage Applications, Publications Office of the European Union, 2018.
[6] W. Zichen, D. Changqing, A comprehensive review on thermal management systems for power lithium–ion batteries, Renew. Sustain. Energy Rev. 139 (2021) 110685.
[7] P.R. Tete, M.M. Gupta, S.S. Joshi, Developments in battery thermal management systems for electric vehicles: A technical review, J. Energy Storage 35 (2021) 102255.
[8] G. Zhao, X. Wang, M. Negnevitsky, H. Zhang, A review of air-cooling battery thermal management systems for electric and hybrid electric vehicles, J. Power Sources 501 (2021) 230001.
[9] A.H. Akinlabi, D. Solyali, Configuration, design, and optimization of air-cooled battery thermal management system for electric vehicles: A review, Renew. Sustain. Energy Rev. 125 (2020) 109815.
[10] L.H. Saw, H.M. Poon, H. San Thiam, Z. Cai, W.T. Chong, N.A. Pambudi, Y.J. King, Novel thermal management system using mist cooling for lithium–ion battery packs, Appl. Energy 223 (2018) 146–158.
[11] R. Zhao, J. Liu, J. Gu, L. Zhai, F. Ma, Experimental study of a direct evaporative cooling approach for Li-ion battery thermal management, Int. J. Energy Res. 44 (8) (2020) 6660–6673.
[12] R.D. Jilte, R. Kumar, L. Ma, Thermal performance of a novel confined flow Li-ion battery module, Appl. Therm. Eng. 146 (2019) 1–11.

[13] W. Li, A. Jishnu, A. Garg, M. Xiao, X. Peng, L. Gao, Heat transfer efficiency enhancement of lithium–ion battery packs by using novel design of herringbone fins, J. Electrochem. Energy Convers. Storage 17 (2) (2020) 021108.
[14] X. Na, H. Kang, T. Wang, Y. Wang, Reverse layered air flow for Li-ion battery thermal management, Appl. Therm. Eng. 143 (2018) 257–262.
[15] J. Zhao, Z. Rao, Y. Huo, X. Liu, Y. Li, Thermal management of cylindrical power battery module for extending the life of new energy electric vehicles, Appl. Therm. Eng. 85 (2015) 33–43.
[16] T. Yang, N. Yang, X. Zhang, G. Li, Investigation of the thermal performance of axial-flow air cooling for the lithium–ion battery pack, Int. J. Therm. Sci. 108 (2016) 132–144.
[17] E. Jiaqiang, M. Yue, J. Chen, H. Zhu, Y. Deng, Y. Zhu, F. Zhang, M. Wen, B. Zhang, S. Kang, Effects of the different air cooling strategies on cooling performance of a lithium–ion battery module with baffle, Appl. Therm. Eng. 144 (2018) 231–241.
[18] S. Shahid, M. Agelin-Chaab, Development and analysis of a technique to improve air-cooling and temperature uniformity in a battery pack for cylindrical batteries, Therm. Sci. Eng. Prog. 5 (2018) 351–363.
[19] R. Mahamud, C. Park, Reciprocating air flow for Li-ion battery thermal management to improve temperature uniformity, J. Power Sources 196 (13) (2011) 5685–5696.
[20] Y. Zhang, X. Song, C. Ma, D. Hao, Y. Chen, Effects of the structure arrangement and spacing on the thermal characteristics of Li-ion battery pack at various discharge rates, Appl. Therm. Eng. 165 (2020) 114610.
[21] N. Yang, X. Zhang, G. Li, D. Hua, Assessment of the forced air-cooling performance for cylindrical lithium–ion battery packs: A comparative analysis between aligned and staggered cell arrangements, Appl. Therm. Eng. 80 (2015) 55–65.
[22] Y. Fan, Y. Bao, C. Ling, Y. Chu, X. Tan, S. Yang, Experimental study on the thermal management performance of air cooling for high energy density cylindrical lithium–ion batteries, Appl. Therm. Eng. 155 (2019) 96–109.
[23] Z. Wang, W. Fan, P. Liu, Simulation of temperature field of lithium battery pack based on computational fluid dynamics, Energy Procedia 105 (2017) 3339–3344.
[24] P. Saechan, I. Dhuchakallaya, Numerical investigation of air cooling system for a densely packed battery to enhance the cooling performance through cell arrangement strategy, Int. J. Energy Res. 46 (14) (2022) 20670–20684.
[25] A. Moosavi, A.-L. Ljung, T.S. Lundström, Design considerations to prevent thermal hazards in cylindrical lithium–ion batteries: An analytical study, J. Energy Storage 38 (2021) 102525.
[26] S.M. Hosseini Moghaddam, Designing Battery Thermal Management Systems (BTMS) for Lithium–ion Battery Modules Using CFD, (M.Sc. thesis), KTH Royal Institute of Technology, Sweden, 2018.
[27] Q. Wang, B. Jiang, B. Li, Y. Yan, A critical review of thermal management models and solutions of lithium–ion batteries for the development of pure electric vehicles, Renew. Sustain. Energy Rev. 64 (2016) 106–128.
[28] M. Zolot, A.A. Pesaran, M. Mihalic, Thermal evaluation of toyota prius battery pack, SAE Tech. Pap. (2002) 01–1962.
[29] T.O. Forslund, I.S. Larsson, H. Lycksam, J.G.I. Hellström, T.S. Lundström, Non-Stokesian flow through ordered thin porous media imaged by tomographic-PIV, Exp. Fluids 62 (2021) 1–12.
[30] A. Žkauskas, Heat transfer from tubes in crossflow, in: Advances in Heat Transfer, vol. 18, Elsevier, 1987, pp. 87–159.
[31] ESDU, Convective heat transfer during crossflow of fluids over plain tube bank, Eng. Sci. Data Unit Item 73031 (1973).
[32] D. Weaver, M. El-Kashlan, On the number of tube rows required to study cross-flow induced vibrations in tube banks, J. Sound Vib. 75 (2) (1981) 265–273.
[33] A. Moosavi, A.-L. Ljung, T.S. Lundström, A comparative study on thermo-fluid characteristics of free and wall-bounded cross-flow heat exchangers, Therm. Sci. Eng. Prog. 40 (2023) 101746.
[34] V. Gnielinski, Equations for calculating heat transfer in single tube rows and banks of tubes in transverse flow, Int. Chem. Eng. 19 (3) (1979) 380–390.
[35] N. Yang, X. Zhang, B. Shang, G. Li, Unbalanced discharging and aging due to temperature differences among the cells in a lithium–ion battery pack with parallel combination, J. Power Sources 306 (2016) 733–741.